Δr and the W-boson mass in the singlet extension of the standard model

D. López-Val[1,*] and T. Robens[2,†]

[1]*Center for Cosmology, Particle Physics and Phenomenology CP3, Université Catholique de Louvain, Chemin du Cyclotron 2, B-1348 Louvain-la-Neuve, Belgium*
[2]*IKTP, Technische Universität Dresden, Zellescher Weg 19, D-01069 Dresden, Germany*

The link between the electroweak gauge boson masses and the Fermi constant via the muon lifetime measurement is instrumental for constraining and eventually pinning down new physics. We consider the simplest extension of the standard model with an additional real scalar $SU(2)_L \otimes U(1)_Y$ singlet and compute the electroweak precision parameter Δr, along with the corresponding theoretical prediction for the W-boson mass. When confronted with the experimental W-boson mass measurement, our predictions impose limits on the singlet model parameter space. We identify regions, especially in the mass range which is accessible by the LHC, where these correspond to the most stringent experimental constraints that are currently available.

I. INTRODUCTION

The relation between the electroweak (EW) gauge boson masses, the Fermi constant $[G_F]$ and the fine structure constant $[\alpha_{\mathrm{em}}]$ is anchored experimentally via the muon lifetime measurement and constitutes a prominent tool for testing the quantum structure of the Standard Model (SM) and its manifold conceivable extensions. This relation is conventionally expressed in the literature by means of the Δr parameter [1–6] and plays a major role in placing bounds on, and eventually unveiling new physics coupled to the standard electroweak Lagrangian.

Aside from being interesting on its own, the quantum effects traded by Δr are part of the electroweak radiative corrections to production and decay processes in the SM and beyond. In particular, the knowledge of Δr is a required footstep toward a full one-loop electroweak characterization of the Higgs boson decay modes in the singlet extension of the SM [7].

The calculation of electroweak precision observables (EWPO) and its role in constraining manifold extensions of the SM has been object of dedicated attention in the literature [1,2,5,6,8–19], including in particular the singlet extension of the SM, cf. e.g. Refs. [20–31].[1] Theoretical predictions for Δr and for the W-boson mass $[m_W^{\mathrm{th}}]$ were first derived in the context of the SM [33,34] and later on extended to new physics models such as the Two-Higgs–Doublet Model (2HDM) [35–43] and the Minimal Supersymmetric Standard Model (MSSM) [17,44–52]. These predictions have proven to be relevant not only to impose parameter space constraints, but also to identify new physics structures capable to in part reconcile the

well-known tension between the SM prediction and the experimental value, $|m_W^{\mathrm{SM}} - m_W^{\mathrm{exp}}| \simeq 20$ MeV. For instance, in Ref. [43] it was shown that the extended Higgs sector of the general 2HDM could yield $m_W^{\mathrm{2HDM}} \gtrsim m_W^{\mathrm{SM}}$, thus potentially alleviating the present discrepancy.

Our main endeavour in this note is to provide a one-loop evaluation of the electroweak parameter Δr and the W-boson mass in the presence of one extra real scalar $SU(2)_L \otimes U(1)_Y$ singlet. This model, which incorporates an additional neutral, CP-even spinless state, corresponds to the simplest renormalizable extension of the SM, and can also be viewed as an effective description of the low-energy Higgs sector of a more fundamental UV completion. Pioneered by Refs. [53–55], this class of models has undergone dedicated scrutiny for the past two decades, revealing rich phenenological implications, especially in the context of collider physics, see e.g. [22,23,25,27,28,30,31,56–66,66–73].

Our starting point is the current most precise theoretical prediction for the SM W-boson mass $[m_W^{\mathrm{SM}}]$, which is known exactly at two-loop accuracy, including up to leading three-loop contributions [49,74–80]. We combine these pure SM effects with the genuine singlet model one-loop contributions and analyze their dependences on the relevant model parameters. Next we correlate our results with the experimental measurement of the W-boson mass and derive constraints on the singlet model parameter space. Finally, we compare them to complementary constraints from direct collider searches, as well as to the more conventional tests based on global fits to electroweak precision observables.

II. Δr AND m_W AS ELECTROWEAK PRECISION MEASUREMENTS

In the so–called "G_F scheme," electroweak precision calculations use the experimentally measured Z-boson

---

*david.lopezval@uclouvain.be
†tania.robens@tu-dresden.de
[1]Cf. also [32], which appeared after the work presented here.

mass [m_Z], the fine-structure constant at zero momentum [$\alpha_{\rm em}(0)$], and the Fermi constant [G_F] as input values. The latter is linked to the muon lifetime via [2,3,5,6]

$$\tau_\mu^{-1} = \frac{G_F^2 m_\mu^5}{192\pi^3} F\left(\frac{m_e^2}{m_\mu^2}\right)\left(1 + \frac{3}{5}\frac{m_\mu^2}{m_W^2}\right)(1 + \Delta_{\rm QED}), \quad (1)$$

where $F(x) = 1 - 8x - 12x^2 \ln x + 8x^3 - x^4$. Following the standard conventions in the literature, the above defining relation for G_F includes the finite QED contributions $\Delta_{\rm QED}$ obtained within the Fermi Model—which are known to two–loop accuracy [81–85]. Matching the muon lifetime in the Fermi model to the equivalent calculation within the full-fledged SM yields the relation:

$$m_W^2\left(1 - \frac{m_W^2}{m_Z^2}\right) = \frac{\pi\alpha_{\rm em}}{\sqrt{2}G_F}(1 + \Delta r) \quad \text{with}$$

$$\Delta r \equiv \frac{\hat\Sigma_W(0)}{m_W^2} + \Delta r^{[\rm vert, box]}, \quad (2)$$

which is the conventional definition of Δr, with $m_{W,Z}$ being the renormalized gauge boson masses in the on-shell scheme. Accordingly, we introduce the on-shell definition of the electroweak mixing angle [33] $\sin^2\theta_W = 1 - m_W^2/m_Z^2$, along with the shorthand notations $s_W^2 \equiv \sin^2\theta_W$, $c_W^2 \equiv 1 - s_W^2$. In turn, $\hat\Sigma_W(k^2)$ denotes the on-shell renormalized W-boson self-energy. The latter accounts for the oblique part of the electroweak radiative corrections to the muon decay. The nonuniversal (i.e. process-dependent) corrections rely on the vertex and box contributions and are subsumed into $\Delta r^{[\rm vert, box]}$. The explicit expression for Δr after renormalization in the on-shell scheme may be written as a combination of loop diagrams and counterterms as follows:

$$\Delta r = \Pi_\gamma(0) - \frac{c_W^2}{s_W^2}\left(\frac{\delta m_Z^2}{m_Z^2} - \frac{\delta m_W^2}{m_W^2}\right) + \frac{\Sigma_W(0) - \delta m_W^2}{m_W^2}$$
$$+ 2\frac{c_W}{s_W}\frac{\Sigma_{\gamma Z}(0)}{m_Z^2} + \Delta r^{[\rm vert, box]}, \quad (3)$$

where $\Pi_\gamma(0)$ stands for the photon vacuum polarization, while $\delta m_{W,Z}^2$ denote the gauge boson mass counterterms. Additional degrees of freedom and/or modified interactions will enter the loop diagrams describing the muon decay, making Δr (and so m_W) model-dependent quantities. At present, the calculation of Δr in the SM is complete up to two loops [49,74–79,86–94] and includes also the leading three [80,95–99] and four-loop pieces [100,101]. The dominant contribution stems from QED fermion loop corrections and is absorbed into the renormalization group running of the fine structure constant.

Taking m_Z and G_F as experimental inputs, and using Eq. (2), the evaluation of Δr within the SM or beyond can be translated into a theoretical prediction for the W-boson mass [$m_W^{\rm th}$]. For this we need to (iteratively) solve the equation

$$m_W^2 = \frac{1}{2}m_Z^2\left[1 + \sqrt{1 - \frac{4\pi\alpha_{\rm em}}{\sqrt{2}G_F m_Z^2}[1 + \Delta r(m_W^2)]}\right]. \quad (4)$$

To first-order accuracy, Eq. (4) implies that a shift $\delta(\Delta r)$ promotes to the W-boson mass through

$$\Delta m_W \simeq -\frac{1}{2}m_W\frac{s_W^2}{c_W^2 - s_W^2}\delta(\Delta r). \quad (5)$$

For $\Delta r = 0$ one retrieves the tree-level value $m_W^{\rm tree} \simeq 80.94$ GeV. But the full theoretical result is smaller in the SM since quantum effects yield $\Delta r > 0$ of order few percent. Once we identify the ~126 GeV resonance with the SM Higgs boson, all experimental input values in Eq. (4) are fixed and thereby the theoretical prediction for the W-boson mass is fully determined. Setting the SM Higgs boson mass to the HIGGSSIGNALS[102–104] best-fit value $m_H = 125.7$ GeV [102], one gets $\Delta r \simeq 0.038 > 0$, wherefrom $m_W^{\rm SM} = 80.360$ GeV. The estimated theoretical uncertainty reads $\Delta m_W^{\rm th} \simeq 4$ MeV [78] and stems mainly from the top mass measurement [105]. This prediction needs to be confronted with the experimental W-boson mass measurement, whose present world-average combines the available results from LEP [106], CDF [107] and D0 [108] and renders

$$m_W^{\rm exp} = 80.385 \pm 0.015 \text{ GeV}. \quad (6)$$

This represents an accuracy at the $\simeq 0.02\%$ level. The corresponding discrepancy with the SM theoretical prediction $|m_W^{\rm exp} - m_W^{\rm SM}| \simeq 20$ MeV falls within the 1σ–level ballpark; however, it is as large as roughly 5 times the estimated theoretical error. On the other hand, these differences should be accessible by the upcoming W-boson mass measurements at the LHC, which are expected to pull the current uncertainty down to $\Delta m_W^{\rm exp} \simeq 10$ MeV [109,110]. Furthermore, a high-luminosity linear collider running in a low-energy mode at the W^+W^- threshold should be able to reduce it even further, namely at the level of $\Delta m_W^{\rm exp} \simeq 5$ MeV or even below [111]. This strongly justifies, if not simply demands, precision calculations of Δr and m_W to probe, constrain, or even unveil, new physics structures linked to the electroweak sector of the SM.

As a byproduct, the task of computing Δr involves the evaluation of the so-called $\delta\rho$ parameter [112–115]. The latter is defined upon the static contribution to the gauge boson self-energies,

$$\frac{\Sigma_Z(0)}{m_Z^2} - \frac{\Sigma_W(0)}{m_W^2} \equiv \delta\rho, \quad (7)$$

and measures the ratio of the neutral-to-charged weak current strength. Quantum effects yielding $\delta\rho \neq 0$ may be traced back to the mass splitting between the partners of a given weak isospin doublet, and so to the degree of departure from the global custodial $SU(2)$ invariance of the SM Lagrangian. The $\delta\rho$ parameter is finite for each doublet of SM matter fermions and is dominated by the top quark loops

$$\delta\rho_{\text{SM}}^{[t]} = \frac{3 G_F m_t^2}{8\sqrt{2}\pi^2}.$$ (8)

In terms of $\delta\rho$, the general expression for Δr can be recast as [2,5,6]:

$$\Delta r = \Delta\alpha - \frac{c_W^2}{s_W^2}\delta\rho + \Delta r_{\text{rem}} = \Delta\alpha + \Delta r^{[\delta\rho]} + \Delta r_{\text{rem}},$$ (9)

where $\Delta r^{[\delta\rho]} \equiv -(c_W^2/s_W^2)\delta\rho$ denotes the individual contribution from the static part of the self-energies. The $\Delta\alpha$ piece accounts for the (leading) QED light-fermion corrections, while the so-called "remainder" term $[\Delta r_{\text{rem}}]$ condenses the remaining (though not negligible) effects. In fact, in the SM we have $\Delta\alpha \simeq 0.06$ and $\Delta r_{\text{rem}} \simeq 0.01$, while $\Delta r^{[\delta\rho]} \simeq -0.03$ [3,5,6].

At variance with this significant contribution, the counterpart Higgs boson-mediated effects are comparably milder in the SM and feature a trademark logarithmic dependence on the Higgs mass [113],[2]

$$\delta\rho^{[\text{H}]} \simeq -\frac{3\sqrt{2}G_F m_W^2}{16\pi^2}\frac{s_W^2}{c_W^2}\left\{\ln\frac{m_H^2}{m_W^2} - \frac{5}{6}\right\} + \cdots.$$ (10)

Remarkably, this telltale *screening* behavior does not hold in general for extended Higgs sectors—viz. in the general 2HDM [43].

III. Δr AND m_W IN THE SINGLET MODEL

A. Model parametrization at leading-order

Our starting point is the most general form of the gauge invariant, renormalizable potential involving one real $SU(2)_L \otimes U(1)_Y$ singlet S and one doublet Φ, the latter carrying the quantum numbers of the SM Higgs weak isospin doublet (see e.g. [29,54,55]):

$$\mathcal{L}_s = (\mathcal{D}^\mu\Phi)^\dagger \mathcal{D}_\mu\Phi + \partial^\mu S \partial_\mu S - V(\Phi, S),$$ (11)

with the potential

$$V(\Phi, S) = -\mu_1^2 \Phi^\dagger\Phi - \mu_2^2 S^2$$

$$+ \begin{pmatrix} \Phi^\dagger\Phi & S^2 \end{pmatrix} \begin{pmatrix} \lambda_1 & \frac{\lambda_3}{2} \\ \frac{\lambda_3}{2} & \lambda_2 \end{pmatrix} \begin{pmatrix} \Phi^\dagger\Phi \\ S^2 \end{pmatrix}$$

$$= -\mu_1^2 \Phi^\dagger\Phi - \mu_2^2 S^2 + \lambda_1(\Phi^\dagger\Phi)^2 + \lambda_2 S^4 + \lambda_3 \Phi^\dagger\Phi S^2.$$ (12)

For the sake of simplicity we consider a minimal version of the singlet model, with an additional $\mathcal{Z}_2$ symmetry forbidding additional terms in the potential. We allow both of the scalar fields to acquire a vacuum expectation value (VEV), in which case the $\mathcal{Z}_2$ symmetry is spontaneously broken by the singlet VEV. The breaking of such a discrete symmetry during the electroweak phase transition in the early universe may in principle lead to problematic weak-scale cosmic domain walls [116–118]. However, analyses of the stability and evolution of such topological defects in multiscalar extensions of the SM (cf. e.g. Refs. [119–121]) identify a variety of mechanisms that may sidestep these issues. These can also be evaded by extending this minimal setup with additional $\mathcal{Z}_2$ breaking terms [122], which would nevertheless have no direct impact on our analysis. In this sense, let us emphasize that we interpret the singlet model as the low–energy effective Higgs sector of a more fundamental UV-completion (cf. e.g. a model with an extended gauge group [123,124]), whose specific details are either way not relevant for the purposes of our study.

The neutral components of these fields can be expanded around their respective VEVs as follows:

$$\Phi = \begin{pmatrix} G^\pm \\ \frac{v_d + l^0 + iG^0}{\sqrt{2}} \end{pmatrix} \qquad S = \frac{v_s + s^0}{\sqrt{2}}.$$ (13)

The minimum of the above potential is achieved under the conditions

$$\mu_1^2 = \lambda_1 v_d^2 + \frac{\lambda_3 v_s^2}{2}; \qquad \mu_2^2 = \lambda_2 v_s^2 + \frac{\lambda_3 v_d^2}{2},$$ (14)

while the quadratic terms in the fields generate the mass-squared matrix

$$\mathcal{M}_{ls}^2 = \begin{pmatrix} 2\lambda_1 v_d^2 & \lambda_3 v_d v_s \\ \lambda_3 v_d v_s & 2\lambda_2 v_s^2 \end{pmatrix}.$$ (15)

Requiring this matrix to be positively-defined leads to the stability conditions[3]

$$\lambda_1, \lambda_2 > 0; \qquad 4\lambda_1\lambda_2 - \lambda_3^2 > 0.$$ (16)

---

[2]One should bear in mind that the Higgs boson contribution in the SM $[\delta\rho_{\text{SM}}^{[\text{H}]}]$ is neither UV finite nor gauge invariant on its own, but only in combination with the remaining bosonic contributions.

[3]Cf. e.g. [29] for a more detailed discussion.

The above mass matrix in the gauge basis $\mathcal{M}_{ls}^2$ can be transformed into the (tree-level) mass basis through the rotation $R(\alpha)\mathcal{M}_{ls}^2 R^{-1}(\alpha) = \mathcal{M}_{hH}^2 = \text{diag}(m_{h^0}^2 m_{H^0}^2)$, with

$$R(\alpha) = \begin{pmatrix} \cos\alpha & -\sin\alpha \\ \sin\alpha & \cos\alpha \end{pmatrix} \quad \text{and} \quad \tan(2\alpha) = \frac{\lambda_3 v_d v_s}{\lambda_1 v_d^2 - \lambda_2 v_s^2}. \tag{17}$$

Its eigenvalues then read

$$m_{h^0,H^0}^2 = \lambda_1 v_d^2 + \lambda_2 v_s^2 \mp |\lambda_1 v_d^2 - \lambda_2 v_s^2|\sqrt{1 + \tan^2(2\alpha)}$$
$$\text{with the convention} \quad m_{H^0}^2 > m_{h^0}^2, \tag{18}$$

and correspond to a light $[h^0]$ and a heavy $[H^0]$ $\mathcal{CP}$-even mass-eigenstate. From Eq. (17), we see that both are admixtures of the doublet $[l^0]$ and the singlet $[s^0]$ neutral components

$$h^0 = l^0 \cos\alpha - s^0 \sin\alpha \quad \text{and} \quad H^0 = l^0 \sin\alpha + s^0 \cos\alpha. \tag{19}$$

The Higgs sector in this model is determined by five independent parameters, which can be chosen as

$$m_{h^0}, m_{H^0}, \sin\alpha, v_d, \tan\beta \equiv \frac{v_d}{v_s},$$

where the doublet VEV is fixed in terms of the Fermi constant through $v_d^2 = G_F^{-1}/\sqrt{2}$. Furthermore, we fix one of the Higgs masses to the LHC value of 125.7 GeV; therefore, three parameters of the model are presently not determined by any experimental measurement.

As only the doublet component can couple to the fermions (via ordinary Yukawa interactions) and the gauge bosons (via the gauge covariant derivative), all of the Higgs couplings to SM particles are rescaled universally, yielding

$$g_{xxh} = g_{xxh}^{SM}(1 + \Delta_{xh}) \quad \text{with}$$
$$1 + \Delta_{xh} = \begin{cases} \cos\alpha & h = h^0 \\ \sin\alpha & h = H^0 \end{cases}. \tag{20}$$

B. Calculation details

Let us now focus on the calculation of Δr and m_W in the singlet extension of the SM. The pure SM contributions

$[\Delta r_{SM}]$ and the genuine singlet model effects $[\delta(\Delta r_{sing})]$ can be split into two UV-finite, gauge-invariant subsets and treated separately:

$$\Delta r_{sing} = \Delta r_{SM} + \delta(\Delta r_{sing}). \tag{21}$$

We here include the state-of-the-art Δr_{SM} evaluation, extracted from Eq. (2) and the numerical parametrization given in Ref. [78], which renders the central values

$$m_W^{SM} = 80.360 \text{ GeV} \quad \text{and} \quad \Delta r_{SM} = 37.939 \times 10^{-3}. \tag{22}$$

We set the top-quark mass $[m_t = 173.07 \text{ GeV}]$ and the Z-boson mass $[m_Z = 91.1875 \text{ GeV}]$ at their current best average values [125]. The SM Higgs mass is fixed to the HIGGSSIGNALS best-fit value of 125.7 GeV. This result for Δr_{SM} includes the full set of available contributions, combining the full-fledged two-loop bosonic [79,94] and fermionic [49,78,93] effects, alongside the leading three-loop corrections at $\mathcal{O}(G_F^3 m_t^6)$ and $\mathcal{O}(G_F^2 \alpha_s m_t^4)$ [80].

The genuine singlet model contributions $[\delta(\Delta r_{sing})]$ originate from the Higgs-boson mediated loops building up the weak gauge boson self-energies, which are shown in Fig. 1. This model-dependent part relies on the Higgs masses $[m_{h^0}, m_{H^0}]$ and the mixing angle $[\sin\alpha]$, and we compute it analytically to one-loop order. As the Higgs self-interactions do not feature at one-loop, the results are insensitive to $\tan\beta$.

At this point, care must be taken not to double-count the pure SM Higgs-mediated contributions. To that aim we define $[\delta(\Delta r_{sing})]$ in Eq. (21) upon subtraction of the SM contribution:

$$\delta(\Delta r_{sing}) \equiv \Delta r_{sing}^{[H]} - \Delta r_{SM}^{[H]} \quad \text{where} \quad \Delta r_{SM}^{[H]} = \Delta r_{sing}^{[H]}|_{\sin\alpha=0}, \tag{23}$$

while the superscript [H] selects the Higgs-mediated contributions in each case. In this expression we explicitly identify the SM-like Higgs boson with the lighter of the two mass-eigenstates $[h^0]$, while the second eigenstate $[H^0]$ is assumed to describe a (so far unobserved) heavier Higgs companion. Analogous expressions can be derived for the complementary case $[m_{H^0} = 125.7 \text{ GeV} > m_{h^0}]$, wherein the SM limit corresponds to $\cos\alpha = 0$. The phenomenology of both possibilities is analyzed separately in Sec. III C.
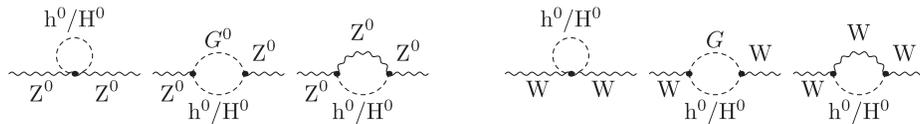

FIG. 1. One-loop Higgs boson-mediated contributions to the weak gauge boson self-energies in the singlet model. The charged and neutral Goldstone boson contributions appear explicitly in the 'tHooft-Feynman gauge. The Feynman diagrams are generated using FEYNARTS.STY [126].

With this in mind, the purely singlet model contributions to the gauge boson self-energies give

$$\bar{\Sigma}_{ZZ}(p^2) = \frac{\alpha_{\rm em}\sin^2\alpha}{4\pi s_W^2 c_W^2}\left\{\frac{[A_0(m_{H^0}^2) - A_0(m_{h^0}^2)]}{4} + m_Z^2[B_0(p^2, m_{H^0}^2, m_Z^2) - B_0(p^2, m_{h^0}^2, m_Z^2)]\right.$$
$$\left. - [B_{00}(p^2, m_{H^0}^2, m_Z^2) - B_{00}(p^2, m_{h^0}^2, m_Z^2)]\right\} \tag{24}$$

$$\bar{\Sigma}_{WW}(p^2) = \frac{\alpha_{\rm em}\sin^2\alpha}{4\pi s_W^2}\left\{\frac{[A_0(m_{H^0}^2) - A_0(m_{h^0}^2)]}{4} + m_W^2[B_0(p^2, m_{H^0}^2, m_W^2) - B_0(p^2, m_{h^0}^2, m_W^2)]\right.$$
$$\left. - [B_{00}(p^2, m_{H^0}^2, m_W^2) - B_{00}(p^2, m_{h^0}^2, m_W^2)]\right\}. \tag{25}$$

The loop integrals in the above equations are expressed in terms of the standard Passarino–Veltman coefficients in the conventions of [127]. The overlined notation $\bar{\Sigma}$ indicates that the overlap with the SM Higgs-mediated contribution has been removed according to Eq. (23). Analogous expressions where $[m_{h^0} \leftrightarrow m_{H^0}]$ and $[\cos\alpha \leftrightarrow \sin\alpha]$ are valid if we identify the heavy scalar eigenstate $[H^0]$ with the SM-like Higgs boson.

The presence of the additional singlet has a twofold impact: (i) first, via the novel one-loop diagrams mediated by the exchange of the additional Higgs boson, as displayed in Fig. 1; (ii) second, via the reduced coupling strength of the SM-like Higgs to the weak gauge bosons, rescaled by the mixing angle [cf. Eq. (20)].

At this stage, we in fact do not yet have to specify a complete renormalization scheme for the model. It suffices to consider the weak gauge boson field and mass renormalization entering Eq. (2). The relevant counterterms therewith are fixed in the on-shell scheme [2,33,128,129], i.e. by requiring the real part of the transverse renormalized self-energies to vanish at the respective gauge boson pole masses, while setting the propagator residues to unity:

$$\mathrm{Re}\hat{\Sigma}_T^W(m_W^2) = 0, \qquad \mathrm{Re}\hat{\Sigma}_T^Z(m_Z^2) = 0,$$
$$\mathrm{Re}\left.\frac{\partial\hat{\Sigma}_T^W(p^2)}{\partial p^2}\right|_{p^2=m_W^2} = 0, \qquad \mathrm{Re}\left.\frac{\partial\hat{\Sigma}_T^Z(p^2)}{\partial p^2}\right|_{p^2=m_Z^2} = 0.$$

The use of the on-shell scheme, which is customary in this context, provides an unambiguous meaning to the free parameters of the model, allowing for a direct mapping between the bare parameters in the classical Lagrangian and the physically measurable quantities in the quantized renormalizable Lagrangian. For instance, choosing on-shell renormalization conditions ensures that the weak gauge boson masses in Eqs. (1)–(2) correspond to their physical masses.[4]

The complete singlet model prediction in Eq. (21) is exact to one-loop order and, as alluded to above, it includes in addition all known higher order SM effects up to leading three-loop precision. Finally, let us also remark that the additional singlet-mediated contributions to the vertex and box diagrams contained in $\Delta r^{[\rm vert, box]}$ [cf. Eq. (3)] are suppressed by the light fermion Yukawa couplings and therefore negligible.

In turn, the static contributions traded by the $\delta\rho$ parameter, as defined in Eq. (7), can be obtained by taking the limit $p^2 \to 0$ on Eqs. (24)–(25) and are given by

$$\Delta(\delta\rho_{\rm sing}) \equiv \delta\rho_{\rm sing}^{[H]} - \delta\rho_{\rm SM}^{[H]} \frac{G_F\sin^2\alpha}{2\sqrt{2}\pi^2}\left\{m_Z^2\left[\log\left(\frac{m_{h^0}^2}{m_{H^0}^2}\right) + \frac{m_Z^2}{m_{h^0}^2 - m_Z^2}\log\left(\frac{m_{h^0}^2}{m_Z^2}\right) - \frac{m_Z^2}{m_{H^0}^2 - m_Z^2}\log\left(\frac{m_{H^0}^2}{m_Z^2}\right)\right.\right.$$
$$\left.+ \frac{m_{H^0}^2}{4(m_{H^0}^2 - m_Z^2)}\log\left(\frac{m_{H^0}^2}{m_Z^2}\right) - \frac{m_{h^0}^2}{4(m_{h^0}^2 - m_Z^2)}\log\left(\frac{m_{h^0}^2}{m_Z^2}\right)\right] - m_W^2\left[\log\left(\frac{m_{h^0}^2}{m_{H^0}^2}\right) + \frac{m_W^2}{m_{h^0}^2 - m_W^2}\log\left(\frac{m_{h^0}^2}{m_W^2}\right)\right.$$
$$\left.\left.- \frac{m_W^2}{m_{H^0}^2 - m_W^2}\log\left(\frac{m_{H^0}^2}{m_W^2}\right) + \frac{m_{H^0}^2}{4(m_{H^0}^2 - m_W^2)}\log\left(\frac{m_{H^0}^2}{m_W^2}\right) - \frac{m_{h^0}^2}{4(m_{h^0}^2 - m_W^2)}\log\left(\frac{m_{h^0}^2}{m_W^2}\right)\right]\right\} \tag{26}$$

---

[4]On-shell mass renormalization in theories with mixing between the gauge eigenstates, as in the Higgs sector of the singlet model, must be nonetheless addressed with care. In these cases, quantum effects generate off-diagonal terms in the loop-corrected propagators, which can be absorbed into the renormalization of the mixing angle. However, it can be shown that, regardless of the specific renormalization scheme chosen for the mixing angle, the on-shell renormalized masses coincide with the physical (pole) masses to one-loop accuracy. A detailed discussion on this issue as well as on the complete renormalization scheme as such for the singlet model will be presented in [7].
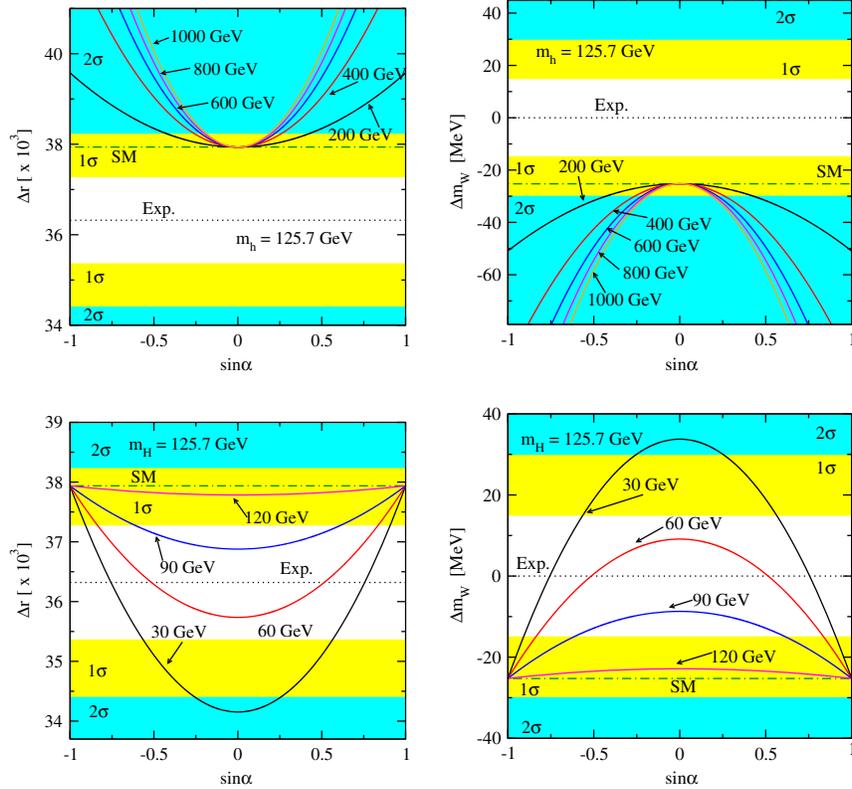
FIG. 2 (color online).   Upper panels: full one–loop evaluation of $\Delta r \equiv \Delta r_{\mathrm{sing}}$ (left) and $\Delta m_W \equiv m_W^{\mathrm{sing}} - m_W^{\mathrm{exp}}$ (right) for different heavy Higgs masses $[m_{\mathrm{H}^0}]$ with fixed $[m_{\mathrm{h}^0} = 125.7 \text{ GeV}]$, as a function of the mixing angle $[\sin\alpha]$. Lower panels: likewise, for different light Higgs masses $[m_{\mathrm{h}^0}]$ and fixed $[m_{\mathrm{H}^0} = 125.7 \text{ GeV}]$. The corresponding SM predictions (the experimental values) are displayed in dashed (dotted) lines. The shaded bands illustrate the 1σ and 2σ C.L. exclusion regions. Compatibility with the LHC signal strength measurements requires $|\sin\alpha| \lesssim 0.42$ (upper panels) and $|\sin\alpha| \gtrsim 0.91$ (lower panels) (cf. Sec. III D).

(cf. also the expression for the T-parameter in the $\overline{\text{MS}}$ scheme [21][5]). The logarithmic dependence on both the light and the heavy Higgs masses follows the same screening-like pattern of the SM, as shown in Eq. (10). The model-specific new physics imprints are again to be found in (i) the additional Higgs contribution; and (ii) the universally rescaled Higgs couplings to the gauge bosons. The size of $\Delta(\delta\rho_{\mathrm{sing}})$ is controlled by the overall factor $\sim \sin^2\alpha$, while its sign, which is fixed by the respective Higgs and gauge boson mass ratios, is negative in all cases. Equation (26) therefore predicts a systematic, negative yield from the new physics effects $[\Delta(\delta\rho_{\mathrm{sing}}) < 0]$, which implies $\delta\rho_{\mathrm{sing}} < \delta\rho_{\mathrm{SM}}$. Finally, and owing to the fact that $\delta\rho$ is linked to Δr via Eq. (9), we may foresee $\Delta r_{\mathrm{sing}} \equiv \Delta r_{\mathrm{SM}} + \delta(\Delta r_{\mathrm{sing}}) > \Delta r_{\mathrm{SM}}$ and hence $m_W^{\mathrm{sing}} < m_W^{\mathrm{SM}}$. Keeping in mind the current $|m_W^{\mathrm{exp}} - m_W^{\mathrm{SM}}| \simeq 20$ MeV (1σ level) tension, this result anticipates tight constraints on the singlet model parameter space—at the level of, if not stronger than, those stemming from the global fits based on

the oblique parameters $[S, T, U]$ [10–12] (cf. discussion in Sec. III D). Conversely, when considering $m_{\mathrm{H}^0} \sim 126$ GeV and a light Higgs companion $[\mathrm{h}^0]$, similar arguments predict a systematic upward shift $[\Delta(\delta\rho_{\mathrm{sing}}) > 0]$ with a global $\cos^2\alpha$ rescaling. In this case, the singlet model has the potential to bring the theoretical value $[m_W^{\mathrm{sing}}]$ closer to the experimental measurement $[m_W^{\mathrm{exp}}]$. In the next subsection we quantitatively justify all these statements.

C. Numerical analysis

In the following we present an upshot of our numerical analysis. Figures 2 and 3 illustrate the behavior of $\Delta r \equiv \Delta r_{\mathrm{sing}}$ and $\Delta m_W \equiv m_W^{\mathrm{sing}} - m_W^{\mathrm{exp}}$ under variations of the relevant singlet model parameters. In Fig. 2 we portray the evolution of both quantities with the mixing angle, for illustrative Higgs companion masses. In the upper panels the SM-like Higgs particle is identified with the lightest singlet model mass-eigenstate $[\mathrm{h}^0]$. We fix its mass to $m_{\mathrm{h}^0} = 125.7$ GeV and sweep over a heavy Higgs mass range $m_{\mathrm{H}^0} = 200$–1000 GeV. The complementary case $[m_{\mathrm{H}^0} = 125.7 \text{ GeV} > m_{\mathrm{h}^0}]$ is examined in the lower panels, with a variable mass for the second (light) Higgs spanning $m_{\mathrm{h}^0} = 5$–125 GeV. The results shown for Δr are

---

[5]It is easy to check that Eq. (26) is equivalent to Eq. (5.1) of Ref. [21], recalling that in our case we identify m_{h^0} with the SM Higgs mass.
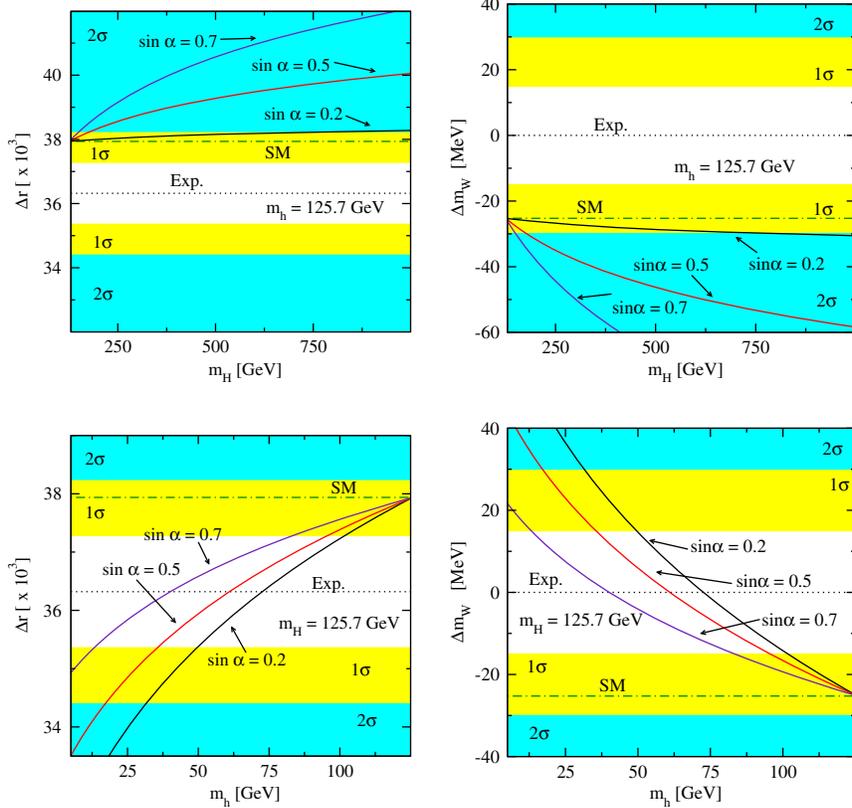
FIG. 3 (color online). Full one–loop evaluation of $\Delta r \equiv \Delta r_{\rm sing}$ (left) and $\Delta m_W \equiv m_W^{\rm sing} - m_W^{\rm exp}$ (right) for different mixing angle values, as a function of the heavy Higgs mass [$m_{\rm H^0}$] (upper panels) and the light Higgs mass [$m_{\rm h^0}$] (lower panels). The corresponding SM predictions (the experimental values) are displayed in dashed (dotted) lines. The shaded bands illustrate the 1σ and 2σ C.L. exclusion regions.

referred to both the SM prediction [$\Delta r_{\rm SM}$] and the experimental value [$\Delta r_{\rm exp}$]. The latter follows from Eq. (2) with the experimental inputs [125]

$$m_W^{\rm exp} = 80.385 \pm 0.015 \text{ GeV}$$

$$m_Z = 91.1876 \pm 0.0021 \text{ GeV}$$

$$\alpha_{\rm em}(0) = 1/137.035999074(44)$$

$$G_F = 1.1663787(6)10^{-5} \text{ GeV}^{-2}, \qquad (27)$$

wherefrom we get

$$\Delta r_{\rm exp} = \frac{\sqrt{2} G_F}{\pi \alpha_{\rm em}} m_W^2 \left(1 - \frac{m_W^2}{m_Z^2}\right) - 1$$

$$= (36.320 \pm 0.976) \times 10^{-3}. \qquad (28)$$

The 1σ and 2σ C.L. regions in $\Delta r_{\rm exp}$ are derived from the $m_W^{\rm exp}$ uncertainty bands using standard error propagation.

Figure 3 provides a complementary view of the Δr and Δm_W dependence on the additional Higgs boson mass assuming mild ($\sin \alpha = 0.2$), moderate ($\sin \alpha = 0.5$) and strong ($\sin \alpha = 0.7$) mixing.

These plots nicely illustrate the parameter dependences anticipated earlier e.g. in Eqs. (24)–(25). On the one hand, the quadratic $\sin^2 \alpha$ ($\cos^2 \alpha$) dependence reflects the global rescaling of the light (heavy) SM-like Higgs coupling to the weak gauge bosons. Accordingly, the values of Δr and $m_W^{\rm sing}$ converge to the SM predictions in the limit $\sin \alpha = 0$ ($\sin \alpha = \pm 1$) in which the new physics effects decouple. The growing departure from the SM as we raise (lower) the mass of the heavy (lighter) Higgs companion follows the logarithmic behavior singled out in Eq. (26), and can be traced back to the increasing breaking of the (approximate) custodial invariance.

In the case where $m_{\rm h^0} = 125.7$ GeV and $m_{\rm H^0} > 130$ GeV (cf. upper panels of Figs. 2 and 3), we pin down positive (negative) deviations of $\Delta r_{\rm sing}$ ($m_W^{\rm sing}$) with respect to the corresponding SM predictions. These increase systematically for larger mixing angles and heavier Higgs companions. The stark dependence on $\sin \alpha$ and $m_{\rm H^0}$, combined with the fact that $m_W^{\rm sing} - m_W^{\rm SM} < 0$ and that $m_W^{\rm SM}$ already lies 20 GeV below the experimental measurement, explains why the results obtained in this case can easily lie outside of the 2σ C.L. exclusion region. In the complementary scenario (cf. lower panels), in which we

TABLE I. Parameter space survey of the electroweak parameters $\Delta r_{\rm sing}$, $\Delta m_W \equiv m_W^{\rm sing} - m_W^{\rm exp}$ and $\delta\rho \equiv \Delta(\delta\rho_{\rm sing})$ in the singlet model for representative Higgs masses and mixing angle choices.

	$\Delta r_{\rm sing}[\times 10^3]$			$m_W^{\rm sing} - m_W^{\rm exp}$ [MeV]			$\Delta(\delta\rho_{\rm sing})[\times 10^4]$		
	h^0 SM-like [$m_{h^0} = 125.7$ GeV]								
m_{H^0} [GeV]	300	500	1000	300	500	1000	300	500	1000
$\sin\alpha = 0.2$	38.067	38.153	38.277	−27	−29	−31	−0.241	−0.428	−0.711
$\sin\alpha = 0.5$	38.744	39.281	40.056	−38	−46	−58	−1.508	−2.674	−4.450
$\sin\alpha = 0.7$	39.515	40.565	42.077	−50	−66	−90	−2.956	−5.244	−8.730
	H^0 SM-like [$m_{H^0} = 125.7$ GeV]								
m_{h^0} [GeV]	30	60	90	30	60	90	30	60	90
$\sin\alpha = 0.2$	34.305	35.824	36.921	31	8	−9	3.798	2.707	1.466
$\sin\alpha = 0.5$	35.103	36.288	37.144	19	1	−13	2.968	2.115	1.146
$\sin\alpha = 0.7$	36.012	36.816	37.398	5	−8	−17	2.019	1.439	0.779

set $m_{H^0} = 125.7$ GeV and vary the light Higgs mass $m_{h^0} \leq 125$ GeV, we find analogous trends—but with interchanged dependences. Here the additional one-loop effects from the light Higgs companion help to release the $m_W^{\rm sing} - m_W^{\rm exp}$ tension. On the other hand, the onset of 2σ-level constraints appears for $m_{h^0} \lesssim 30$ GeV. These results spotlight a significant mass range in which the singlet model contributions could in principle achieve $m_W^{\rm sing} \simeq m_W^{\rm exp}$.[6] The viability of these scenarios is nevertheless hindered in practice, due to the direct collider mass bounds and the LHC signal strength measurements. The impact of these additional constraints, which at this point we have not yet included, will be addressed in Sec. III D[7]

Our discussion is complemented by specific numerical predictions for Δr and $m_W^{\rm sing} - m_W^{\rm exp}$, which we list in Table I for representative parameter choices. For small mixing $|\sin\alpha| \lesssim 0.2$ and heavy Higgs masses of few hundred GeV, $\Delta r_{\rm sing}$ departs from $\Delta r_{\rm SM}$ at the $\mathcal{O}(0.1)\%$ level. These deviations may increase up to $\mathcal{O}(10)\%$ for mixing angles above $|\sin\alpha| \gtrsim 0.5$ and $\mathcal{O}(1)$ TeV scalar companions. Not surprisingly, these are the parameter space configurations that maximize the non–standard singlet model imprints, viz. the rescaled Higgs boson interactions and the non-decoupling mass dependence of the Higgs-mediated loops. As we have seen in Figs. 2–3, and according to Eq. (5), these shifts pull the resulting prediction [$m_W^{\rm sing}$] down to ~1–70 MeV below the SM result. Staying within 1σ C.L. we find $|m_W^{\rm sing} - m_W^{\rm SM}| \simeq 10$ MeV ($m_W^{\rm sing} < m_W^{\rm SM}$) for relatively tempered mixing ($|\sin\alpha| \lesssim 0.2$) and heavy Higgs masses up to 1 TeV. Larger mixings of typically

$|\sin\alpha| \gtrsim 0.4$ push $m_W^{\rm sing}$ into the 2σ-level exclusion region. These results once more illustrate that, for a second *heavy* Higgs resonance, the singlet model effects tend to sharpen the $m_W^{\rm th} - m_W^{\rm exp}$ tension even further, and more so as we increasingly depart from the SM–like limit. Alternatively, for $m_{h^0} < m_{H^0} = 125.7$ GeV we find that relative deviations of ~5% in $\Delta r_{\rm sing}$ (with $\Delta r_{\rm sing} < \Delta r_{\rm SM}$) are attainable for 50–100 GeV light Higgs companion masses and mixing angles above $|\sin\alpha| \sim 0.5$.

Alongside with the calculation of Δr and $m_W^{\rm sing}$ we compute the new physics one-loop contributions to the $\delta\rho$ parameter [cf. Eq. (7)]. The behavior of $\Delta(\delta\rho_{\rm sing})$ as a function of the relevant singlet model parameters [$\sin\alpha$] and [m_{h^0,H^0}] is illustrated in Fig. 4. Again, we separately examine the two complementary situations in which either the lighter (top-row panels) or the heavier (bottom-row panels) singlet model mass-eigenstate describes the SM-like Higgs boson. As expected, $|\Delta(\delta\rho_{\rm sing})|$ enlarges as we progressively separate from the SM limit. The strong dependence in the additional Higgs mass displays the increasing deviation from the custodial symmetry limit, which is enhanced by the mass splitting between the Higgs mass-eigenstates. Conversely, we recover $\Delta(\delta\rho_{\rm sing}) \to 0$ in the $m_{h^0} \to m_{H^0}$ limit. The relative size of the static one-loop effects encapsulated in $\Delta(\delta\rho_{\rm sing})$ is quantified in the lower subpanels of Fig. 4 through the ratio

$$\Delta r_{\rm rel}^{[\delta\rho]} \equiv \Delta r_{\rm sing}^{[\delta\rho]}/\Delta r_{\rm sing} = -c_W^2/s_W^2 \Delta(\delta\rho_{\rm sing})/\Delta r_{\rm sing}, \quad (29)$$

which we construct from the different pieces singled out in Eq. (9), retaining the singlet model contributions only.

Interestingly, the analysis of $\delta\rho$ provides a handle for estimating the size of higher-order corrections. The leading singlet model two-loop effects [$\Delta(\delta\rho_{\rm sing}^{[2]})$] arise from the exchange of virtual top quarks and Higgs bosons. This type of mixed $\mathcal{O}(G_F^2 m_t^4)$ Yukawa corrections was first computed within the SM in the small Higgs boson mass limit in Ref. [131] and later on extended to arbitrary masses

---

[6]Let us recall that both instances $m_W^{\rm th} - m_W^{\rm exp} \lesssim 0$ are possible in the 2HDM for a large variety of Higgs mass spectra. However, unlike the singlet model case, these situations are not attached to a specific mass hierarchy [43].

[7]A fully comprehensive analysis of the model combining all currently available constraints deserves a dedicated study and will be presented elsewhere [130].
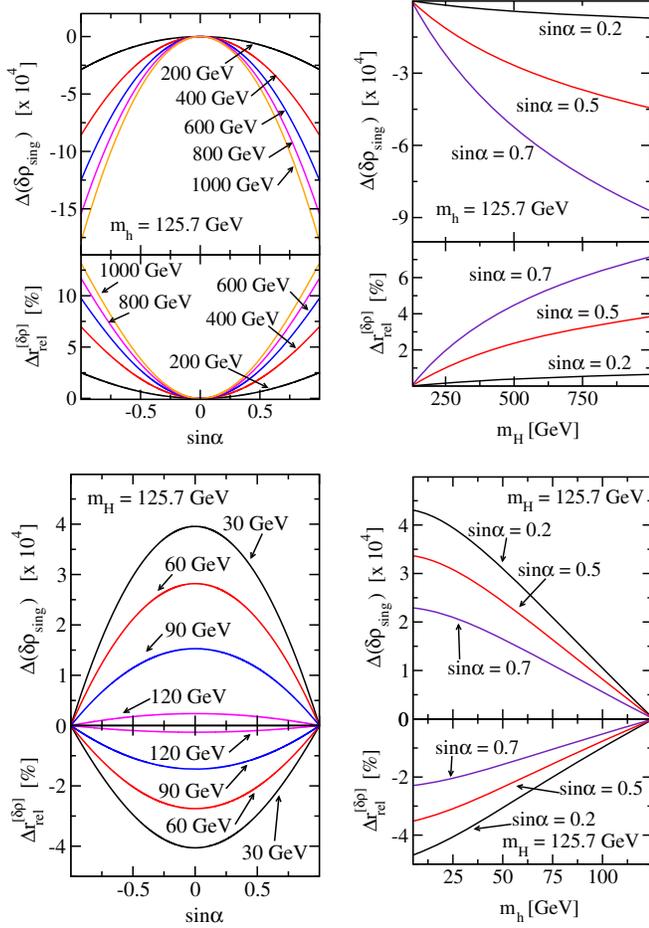
FIG. 4 (color online). Singlet model contribution to the $\delta\rho$ parameter at one loop $[\Delta(\delta\rho_{\mathrm{sing}})]$ for representative mixing angles and Higgs companion masses. In the bottom subpanels we quantify the relative size of these contributions to the overall Δr prediction, following Eq. (29).

[132,133]. The analytical expressions therewith can be readily exported to our case. Taking into account the rescaled top-quark interactions with the light (heavy) Higgs mass-eigenstate by an overall factor $\sim\cos^2\alpha$ ($\sim\sin^2\alpha$); and removing as usual the overlap with the SM contribution (which we identify here with h^0 in the $\sin\alpha = 0$ limit) we find

$$
\Delta(\delta\rho^{[2]}_{\mathrm{sing}}) = \frac{3G_F^2 m_t^4 \sin^2\alpha}{128\pi^4}(f(m_t^2/m_{\mathrm{H}^0}^2) - f(m_t^2/m_{\mathrm{h}^0}^2))
$$
$$
\sim \frac{3G_F^2 m_t^4 \sin^2\alpha}{128\pi^4}\left[27\log\left(\frac{m_t}{m_{\mathrm{H}^0}}\right) + \frac{4\pi m_{\mathrm{h}^0}}{m_t}\right], \quad (30)
$$

where in the latter step we have introduced the asymptotic expansions of $f(r)$ [132,133]. The above estimate $\Delta(\delta\rho^{[2]}_{\mathrm{sing}})$ stagnates around $\mathcal{O}(10^{-4})$ for fiducial parameter choices with $|\sin\alpha| \lesssim 0.5$. When promoted to the W-boson mass prediction through Eqs. (5) and (9) we find

TABLE II. Upper limits on the mixing angle compatible with m_W^{exp} at the 2σ-level, for $m_{\mathrm{h}^0} = 125.7$ GeV and representative heavy Higgs masses. Consistency with the LHC signal strength measurement implies $|\sin\alpha| \leq 0.42$, cf. Fig. 6.

m_H[GeV]	$|\sin\alpha|_{\max}$
1000	0.19
900	0.20
800	0.20
700	0.21
600	0.22
500	0.24
400	0.26
300	0.31
200	0.43
150	0.70
130	1.00

$$
[\Delta(m_W^{[2]})]_{\mathrm{sing}} \sim -\frac{1}{2}m_W\frac{s_W^2}{c_W^2 - s_W^2}\delta(\Delta r_{\mathrm{sing}}^{\delta[\rho]}) \lesssim \mathcal{O}(1)\ \mathrm{MeV},
$$
$$(31)$$

which we can interpreted as an estimate on the theoretical uncertainty on m_W^{sing} due to the quantum effects beyond the one-loop order.

D. Comparison to complementary model constraints

In this section, we first confront the model constraints imposed by the $[m_W^{\mathrm{sing}} - m_W^{\mathrm{exp}}]$ comparison to those following from global fits to electroweak precision data. The difference $[m_W^{\mathrm{sing}} - m_W^{\mathrm{exp}}]$ corresponds to a (pseudo)observable which can directly be linked to a single experimental measurement. The electroweak precision tests are customary expressed in terms of the oblique parameters $[S, T, U]$, cf. e.g. Refs. [20,23,25,26,57,58,66] for analyses of the singlet extension with a $\mathcal{Z}_2$ symmetry, and [21,24] for a slightly different model setup. In the standard conventions [125], and retaining the one–loop singlet model contributions only, these parameters are given by

$$
\frac{\alpha_{\mathrm{em}}}{4s_W^2 c_W^2}S = \frac{\bar{\Sigma}_Z(m_Z^2) - \bar{\Sigma}_Z(0)}{m_Z^2}; \qquad \frac{\alpha_{\mathrm{em}}}{}T = \frac{\bar{\Sigma}_W(0)}{m_W^2} - \frac{\bar{\Sigma}_Z(0)}{m_Z^2};
$$
$$
\frac{\alpha_{\mathrm{em}}}{4s_W^2}U = \frac{\bar{\Sigma}_W(m_W^2) - \bar{\Sigma}_W(0)}{m_W^2} - c_W^2\frac{\bar{\Sigma}_Z(m_Z^2) - \bar{\Sigma}_Z(0)}{m_Z^2}.
$$
$$(32)$$

Notice that genuine singlet model contributions to the photon and the mixed photon–Z vacuum polarization are absent at one loop. The overlined notation $\bar{\Sigma}$ is once more tracking down the consistent subtraction of the overlap with the SM Higgs-mediated contributions, as specified by Eq. (23). The T parameter can obviously be related to the
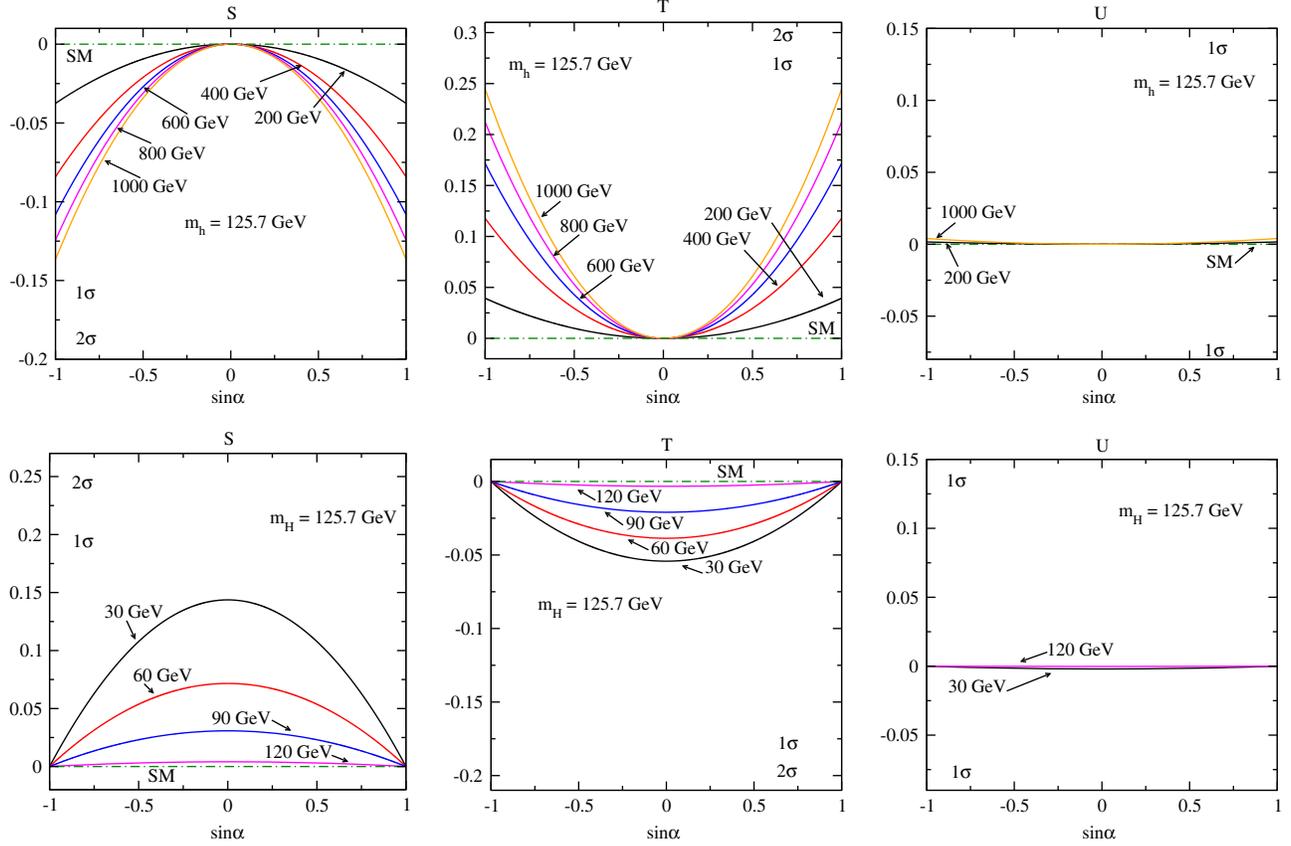
FIG. 5 (color online).   Singlet model contributions to the oblique parameters S (left), T (center) and U (right) as a function of the mixing angle for representative heavy (upper row) and light (lower row) Higgs companion masses. The dashed-dotted line represents the fiducial SM reference value $S, T, U = 0$.

$\delta\rho$ parameter in Eq. (7), yielding $\alpha_{\rm em}T = -\delta\rho$. Likewise, we may rewrite $\Delta r_{\rm sing}$ as

$$\Delta r_{\rm sing} = \frac{\alpha_{\rm em}}{s_W^2}\left(-\frac{1}{2}S + c_W^2 T + \frac{c_W^2 - s_W^2}{4s_W^2}U\right). \quad (33)$$

In Fig. 5 we portray the functional dependence $[S, T, U]$ with respect to the relevant singlet model parameters. The best-fit point has been taken from Ref. [134], including the LHC Higgs mass measurement of 126.7 ± 0.4 GeV as an input parameter, and yields

$$S = 0.03 \pm 0.10; \quad T = 0.05 \pm 0.12; \quad U = 0.03 \pm 0.10. \quad (34)$$

Correlations among these parameters are relevant and must be taken into account when electroweak precision global fit estimates are used to constrain the parameter space of the model. To that aim we here use the best linear unbiased estimator (see e.g. [135]) based on the Gauss–Markov theorem which yields

$$\chi^2 = (\mathcal{O}_l - \hat{\mathcal{O}}_l)(V_{lk})^{-1}(\mathcal{O}_k - \hat{\mathcal{O}}_k) \quad \text{with} \quad \mathcal{O}_l = \{S, T, U\}, \quad (35)$$

where $\hat{\mathcal{O}}_l$ stand for the global best-fit values of the oblique parameters in Eq. (34). The covariance matrix V_{lk} is extracted from Ref. [134], with correlation coefficients between the parameter pairs $[(S, T), (S, U), (T, U)]$ given by $[+0.89, -0.54, -0.83]$ respectively.

We carry out our analysis by fixing the heavy (resp. light) additional scalar mass and allowing for correlated variations of up to 2σ in each of these parameters. For a two-parameter estimate, this translates into $|\Delta\chi| \leq 5.99$. That way we derive upper (resp. lower) mixing angle limits, which correspond to the parameter space regions compatible with these global electroweak precision tests. Albeit rendering non-negligible constraints, we find the resulting limits (cf. e.g. the magenta line of Fig. 6) to be superseded by other constraints throughout the entire parameter space, as we discuss below.

Next, we also consider the constraints to the maximal values of the mixing angle stemming from direct collider searches and the averaged LHC Higgs signal strength
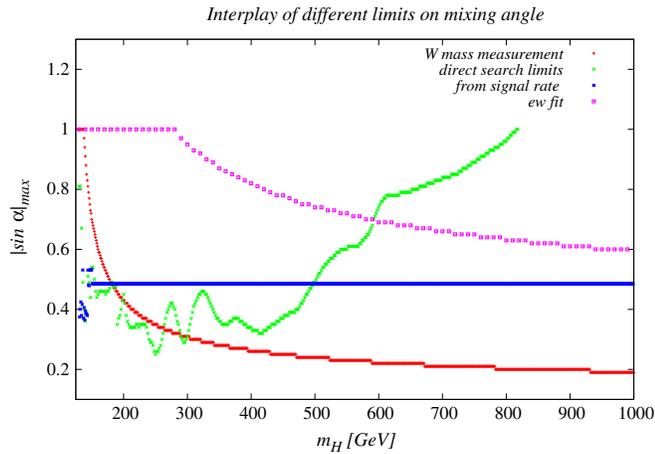
FIG. 6 (color online). Upper limits on the mixing angle $|\sin\alpha|_{max}$ from (i) the m_W^{exp} measurement; (ii) direct collider searches; (iii) compatibility with the $m_{h^0} = 125.7$ GeV LHC Higgs signal strength measurements, and (iv) electroweak precision tests using S, T, U.

measurements $[\bar{\mu}^{exp}]$. For the former, we use HIGGSBOUNDS [136] which incorporates detailed information from around 300 search channels from the LEP, Tevatron, and LHC experiments, to extract upper (resp. lower) limits on the mixing angle $|\sin\alpha|_{max\ (min)}$ as a function of the heavy (resp. light) Higgs companion. In the mass range $m_{H^0} = 200$–1000 GeV, the primary collider limits follow from the CMS four–lepton mode search [137]; for lower masses additional channels are equally important [138,139]. Concerning the Higgs signal strength, we use the most recent values reported in [140,141]

$$\mu_{ATLAS} = 1.30 \pm 0.18, \qquad \mu_{CMS} = 0.80 \pm 0.14$$

$$\text{wherefrom } \bar{\mu}^{exp} = 1.05 \pm 0.11. \qquad (36)$$

A word of caution should be given here. Note that these best-fit estimates and C.L. limits are not tailored to any particular model. This means for instance that, although the singlet model can only yield a suppressed Higgs signal strength $\mu^{sing} \leq 1$, such restriction is not enforced beforehand when deriving the results in Eq. (36). Dedicated model-specific analyses should therefore include such model-dependent fit priors, which would eventually modify the resulting bounds.[8]

To estimate the mixing angle range for which $\bar{\mu}^{sing}$ is compatible with the LHC observations $[\bar{\mu}^{exp}]$, we identify the light (heavy) singlet model mass-eigenstate with the SM Higgs boson and assume a global rescaling $\bar{\mu}^{sing}/\bar{\mu}^{SM} \simeq \cos^2\alpha(\sin^2\alpha)$. In this simple estimate, we do not entertain the possibility that two eigenstates with almost degenerate masses $m_{h^0} \simeq m_{H^0}$ could contribute to the LHC Higgs

---

[8]We thank A. Straessner for clarifying comments regarding this point.

signal. Allowing up to 2σ-level deviations, we obtain upper (lower) mixing angle limits of $|\sin\alpha| \leq 0.42 (|\sin\alpha| \geq 0.91)$. In the latter case, namely for $m_{h^0} < m_{H^0} = 125.7$ GeV, these are in fact comparable to or even stronger than the mass constraints from direct collider searches alone, as well as from the limits on the oblique $[S, T, U]$ parameters. This result implies that the parameter space for the case of $m_{H^0} = 125.7$ GeV $> m_{h^0}$ is severely restricted. Consequently, most regions in Figs. 2–3 for which quantum corrections would shrink the $[m_W^{th} - m_W^{exp}]$ discrepancy below the 1σ-level are in practice precluded by the LHC signal strength measurements. One should also bear in mind that, for very light m_{h^0} masses, additional constraints from low-energy observables may play a significant role, see e.g. [142–144] and references therein.

On the other hand, larger regions of parameter space are still allowed when $m_{h^0} = 125.7$ GeV $< m_{H^0}$. For this case, compared vistas of the different model constraints are displayed in Fig. 6 (see also Table II). We sweep the heavy Higgs masses in the range 130–1000 GeV and overlay the upper bounds on the mixing angle $|\sin\alpha|_{max}$ from each constraint individually. While direct search bounds and signal strength measurements dominate in the low-mass region, both are superseded by the W-boson mass measurement $[m_W^{exp}]$ for $m_{H^0} \gtrsim 300$ GeV. This can once again be attributed to the Higgs-mediated corrections encoded within Δr, which increase with m_{H^0} and are ultimately linked to the custodial symmetry breaking. In turn, the limits imposed by the correlated oblique $[S, T, U]$ parameters (cf. the magenta curve in Fig. 6) are also milder than those obtained from the $[m_W^{sing} - m_W^{exp}]$ comparison. This result is after all not surprising (cf. e.g. Ref. [145]) and reflects the fact in a global fit (in this case parametrized by $[S, T, U]$), the effect of the individual observables involved in it can balance each other in part. The resulting C.L. limits are then smeared with respect to the situation in which we separately consider the more constraining measurements (in our case m_W^{exp}) individually. In this regard, let us recall the very accurate precision (viz. 0.02% level) available for the W-boson mass measurement. We conclude that these different sources of constraints are highly complementary to each other in the different heavy Higgs mass regions, and in all cases rule out substantial deviations from the SM-like limit, viz. mixing angles of $|\sin\alpha| \gtrsim 0.2$–0.4.

IV. SUMMARY

We have reported on the computation of the electroweak precision parameter Δr, along with the theoretical prediction of the W-boson mass, in the presence of one additional real scalar $SU(2)_L \otimes U(1)_Y$ singlet. The Δr parameter trades the relation between the electroweak gauge boson masses, the Fermi constant and the muon lifetime. Its precise theoretical knowledge plays a salient role in the quest for physics beyond the SM. The reason is twofold:

first, because Δr and m_W constitute a probe of electroweak quantum effects and are therefore sensitive to, and able to constrain, extended Higgs sectors; and second, due to the current 1σ discrepancy $|m_W^{\rm SM} - m_W^{\rm exp}| \sim 20$ MeV which, if eventually growing with the more accurate upcoming W-boson mass measurements, it could become a smoking gun for new physics.

In this work we have combined the state-of-the-art SM prediction (available up to leading three-loop accuracy) with the one–loop evaluation of the genuine singlet model effects. The two possible realizations of the singlet-extended SM Higgs sector, viz. featuring a heavy or a light Higgs companion, have been separately examined. Finally, we have confronted the constraints on the parameter space stemming from $[m_W^{\rm exp}]$ to the limits imposed by (i) direct collider searches; (ii) Higgs signal strength measurements; and (iii) the bounds on $[S, T, U]$ based on global fits to electroweak precision data.

Our conclusions may be outlined as follows:

(i) The singlet model contributions to Δr and m_W are characterized by: (i) a global rescaling factor which depends on the mixing between the two scalar mass-eigenstates and reflects the universal suppression of all Higgs boson couplings in this model; (ii) the additional exchange of the second Higgs boson, which exhibits a logarithmic screening-like non-decoupling dependence with the Higgs mass.

(ii) The singlet-induced new physics effects may typically yield up to $\mathcal{O}(10)\%$ deviations in the Δr parameter with respect to the SM prediction. Due to the characteristic dependence on the Higgs masses, these departures are bound to be positive if the lightest mass eigenstate is identified with the SM Higgs boson. Such a shift $\Delta r_{\rm sing} > \Delta r_{\rm SM}$ implies $|m_W^{\rm sing} - m_W^{\rm SM}| \sim 1$–70 MeV with $m_W^{\rm sing} < m_W^{\rm SM}$, which raises the tension with the current $[m_W^{\rm exp}]$ measurement. These trends are reverted if we exchange the roles of the two mass-eigenstates

and consider instead a light Higgs companion with $m_{h^0} < m_{H^0} = 125.7$ GeV. In that case we retrieve $\Delta r_{\rm sing} < \Delta r_{\rm SM}$ and hence $m_W^{\rm sing} > m_W^{\rm SM}$, which makes in principle possible to satisfy $m_W^{\rm sing} \simeq m_W^{\rm exp}$. The viability of these scenarios is nonetheless limited in practice, as they are hardly compatible with the Higgs signal strength measurements.

(iii) Tight upper bounds on the mixing angle parameter $|\sin \alpha|_{\rm max}$ can be derived when confronting $[m_W^{\rm sing}]$ to $[m_W^{\rm exp}]$. These are particularly stringent for $m_{h^0} = 125.7$ GeV and $m_{H^0} \gtrsim 300$ GeV, and reflect the enhanced breaking of the (approximate) custodial symmetry of the SM. In fact, in this mass range they dominate over the additional model constraints from direct collider searches and Higgs signal strength measurements, as well as from global electroweak fits traded by the oblique parameters $[S, T, U]$.

With the calculation of the Δr parameter, we have taken one step towards a complete characterization of the one-loop electroweak effects in the singlet extension of the SM. The knowledge of Δr is a key element in the evaluation of the electroweak quantum corrections to the Higgs boson decays. Work in this direction is underway [7].

ACKNOWLEDGMENTS

[1] D. Kennedy and B. Lynn, Nucl. Phys. **B322**, 1 (1989).
[2] W. Hollik, Fortsch. Phys. **38**, 165 (1990).
[3] W. Hollik, in *Precision tests of the standard electroweak model*, edited by P. Langacker (1993), pp. 37–116.
[4] P. Langacker, in Advanced Series on Directions in High Energy Physics Vol. 14 (World Scientific, Singapore, 1995), p. 1008.
[5] W. Hollik, J. Phys. G **29**, 131 (2003).
[6] W. Hollik, J. Phys. Conf. Ser. **53**, 7 (2006).
[7] D. López-Val and T. Robens (to be published).
[8] J. Grifols and J. Solà, Phys. Lett. **137B**, 257 (1984).
[9] J. Grifols and J. Solà, Nucl. Phys. **B253**, 47 (1985).
[10] M. E. Peskin and T. Takeuchi, Phys. Rev. Lett. **65**, 964 (1990).
[11] M. E. Peskin and T. Takeuchi, Phys. Rev. D **46**, 381 (1992).
[12] I. Maksymyk, C. Burgess, and D. London, Phys. Rev. D **50**, 529 (1994).
[13] G. Altarelli and R. Barbieri, Phys. Lett. B **253**, 161 (1991).
[14] G. Altarelli, R. Barbieri, and S. Jadach, Nucl. Phys. **B369**, 3 (1992).
[15] D. Garcia, R. A. Jiménez, and J. Solà, Phys. Lett. B **347**, 309 (1995).

[16] D. Garcia, R. A. Jiménez, and J. Solà, Phys. Lett. B **347,** 321 (1995).

[17] S. Heinemeyer, W. Hollik, and G. Weiglein, Phys. Rep. **425,** 265 (2006).

[18] J. D. Wells, arXiv:hep-ph/0512342.

[19] A. Sirlin and A. Ferroglia, Rev. Mod. Phys. **85,** 263 (2013).

[20] M. Bowen, Y. Cui, and J. D. Wells, J. High Energy Phys. 03 (2007) 036.

[21] S. Profumo, M. J. Ramsey-Musolf, and G. Shaughnessy, J. High Energy Phys. 08 (2007) 010.

[22] V. Barger, P. Langacker, M. McCaskey, M. J. Ramsey-Musolf, and G. Shaughnessy, Phys. Rev. D **77,** 035005 (2008).

[23] S. Dawson and W. Yan, Phys. Rev. D **79,** 095002 (2009).

[24] J. M. Cline, G. Laporte, H. Yamashita, and S. Kraml, J. High Energy Phys. 07 (2009) 040.

[25] C. Englert, T. Plehn, D. Zerwas, and P. M. Zerwas, Phys. Lett. B **703,** 298 (2011).

[26] R. S. Gupta, H. Rzehak, and J. D. Wells, Phys. Rev. D **86,** 095001 (2012).

[27] D. Bertolini and M. McCullough, J. High Energy Phys. 12 (2012) 118.

[28] M. J. Dolan, C. Englert, and M. Spannowsky, Phys. Rev. D **87,** 055002 (2013).

[29] G. M. Pruna and T. Robens, Phys. Rev. D **88,** 115012 (2013).

[30] C. Englert and M. McCullough, J. High Energy Phys. 07 (2013) 168.

[31] R. S. Chivukula, A. Farzinnia, J. Ren, and E. H. Simmons, Phys. Rev. D **88,** 075020 (2013).

[32] S. Profumo, M. J. Ramsey-Musolf, C. L. Wainwright, and P. Winslow, arXiv:1407.5342.

[33] A. Sirlin, Phys. Rev. D **22,** 971 (1980).

[34] W. Marciano and A. Sirlin, Phys. Rev. D **22,** 2695 (1980).

[35] J. Frère and J. Vermaseren, Z. Phys. C **19,** 63 (1983).

[36] S. Bertolini, Nucl. Phys. **B272,** 77 (1986).

[37] W. Hollik, Z. Phys. C **32,** 291 (1986).

[38] W. Hollik, Z. Phys. C **37,** 569 (1988).

[39] C. Froggatt, R. Moorhouse, and I. Knowles, Phys. Rev. D **45,** 2471 (1992).

[40] H.-J. He, N. Polonsky, and S.-f. Su, Phys. Rev. D **64,** 053004 (2001).

[41] W. Grimus, L. Lavoura, O. Ogreid, and P. Osland, J. Phys. G **35,** 075001 (2008).

[42] W. Grimus, L. Lavoura, O. Ogreid, and P. Osland, Nucl. Phys. **B801,** 81 (2008).

[43] D. López-Val and J. Solà, Eur. Phys. J. C **73,** 2393 (2013).

[44] J. van der Bij and M. Veltman, Nucl. Phys. **B231,** 205 (1984).

[45] R. Barbieri, M. Frigeni, F. Giuliani, and H. Haber, Nucl. Phys. **B341,** 309 (1990).

[46] P. Gosdzinsky and J. Solà, Mod. Phys. Lett. A **06,** 1943 (1991).

[47] D. Garcia and J. Solà, Mod. Phys. Lett. A **09,** 211 (1994).

[48] P. H. Chankowski, A. Dabelstein, W. Hollik, W. M. Mösle, S. Pokorski, and J. Rosiek, Nucl. Phys. **B417,** 101 (1994).

[49] A. Freitas, W. Hollik, W. Walter, and G. Weiglein, Nucl. Phys. **B632,** 189 (2002).

[50] S. Heinemeyer and G. Weiglein, J. High Energy Phys. 10 (2002) 072.

[51] S. Heinemeyer, W. Hollik, D. Stöckinger, A. Weber, and G. Weiglein, J. High Energy Phys. 08 (2006) 052.

[52] S. Heinemeyer, W. Hollik, G. Weiglein, and L. Zeune, J. High Energy Phys. 12 (2013) 084.

[53] V. Silveira and A. Zee, Phys. Lett. **161B,** 136 (1985).

[54] R. Schabinger and J. D. Wells, Phys. Rev. D **72,** 093007 (2005).

[55] B. Patt and F. Wilczek, arXiv:hep-ph/0605188.

[56] D. O'Connell, M. J. Ramsey-Musolf, and M. B. Wise, Phys. Rev. D **75,** 037701 (2007).

[57] O. Bahat-Treidel, Y. Grossman, and Y. Rozen, J. High Energy Phys. 05 (2007) 022.

[58] G. Bhattacharyya, G. C. Branco, and S. Nandi, Phys. Rev. D **77,** 117701 (2008).

[59] M. Gonderinger, Y. Li, H. Patel, and M. J. Ramsey-Musolf, J. High Energy Phys. 01 (2010) 053.

[60] S. Bock, R. Lafaye, T. Plehn, M. Rauch, D. Zerwas, and P. M. Zerwas, Phys. Lett. B **694,** 44 (2010).

[61] P. J. Fox, D. Tucker-Smith, and N. Weiner, J. High Energy Phys. 06 (2011) 127.

[62] C. Englert, J. Jaeckel, E. Re, and M. Spannowsky, Phys. Rev. D **85,** 035008 (2012).

[63] B. Batell, S. Gori, and L.-T. Wang, J. High Energy Phys. 06 (2012) 172.

[64] C. Englert, T. Plehn, M. Rauch, D. Zerwas, and P. M. Zerwas, Phys. Lett. B **707,** 512 (2012).

[65] R. S. Gupta and J. D. Wells, Phys. Lett. B **710,** 154 (2012).

[66] B. Batell, D. McKeen, and M. Pospelov, J. High Energy Phys. 10 (2012) 104.

[67] F. Bazzocchi and M. Fabbrichesi, Eur. Phys. J. C **73,** 2303 (2013).

[68] D. López-Val, T. Plehn, and M. Rauch, J. High Energy Phys. 10 (2013) 134.

[69] S. Heinemeyer et al. (LHC Higgs Cross Section Working Group), arXiv:1307.1347.

[70] B. Cooper, N. Konstantinidis, L. Lambourne, and D. Wardrope, Phys. Rev. D **88,** 114005 (2013).

[71] C. Caillol, B. Clerbaux, J.-M. Frère, and S. Mollet, Eur. Phys. J. Plus **129,** 93 (2014).

[72] R. Coimbra, M. O. Sampaio, and R. Santos, Eur. Phys. J. C **73,** 2428 (2013).

[73] A. Eichhorn and M. M. Scherer, Phys. Rev. D **90,** 025023 (2014).

[74] A. Freitas, S. Heinemeyer, and G. Weiglein, Nucl. Phys. B, Proc. Suppl. **116,** 331 (2003).

[75] M. Awramik and M. Czakon, Phys. Rev. Lett. **89,** 241801 (2002).

[76] M. Awramik, M. Czakon, A. Onishchenko, and O. Veretin, Phys. Rev. D **68,** 053004 (2003).

[77] M. Awramik and M. Czakon, Phys. Lett. B **568,** 48 (2003).

[78] M. Awramik, M. Czakon, A. Freitas, and G. Weiglein, Phys. Rev. D **69,** 053006 (2004).

[79] A. Onishchenko and O. Veretin, Phys. Lett. B **551,** 111 (2003).

[80] J. van der Bij, K. Chetyrkin, M. Faisst, G. Jikia, and T. Seidensticker, Phys. Lett. B **498,** 156 (2001).

[81] R. Behrends, R. Finkelstein, and A. Sirlin, Phys. Rev. **101,** 866 (1956).

[82] T. Kinoshita and A. Sirlin, Phys. Rev. **113,** 1652 (1959).

[83] T. van Ritbergen and R. G. Stuart, Nucl. Phys. **B564**, 343 (2000).

[84] M. Steinhauser and T. Seidensticker, Phys. Lett. B **467**, 271 (1999).

[85] A. Pak and A. Czarnecki, Phys. Rev. Lett. **100**, 241807 (2008).

[86] A. Djouadi and C. Verzegnassi, Phys. Lett. B **195**, 265 (1987).

[87] A. Djouadi, Nuovo Cimento Soc. Ital. Fis. **100A**, 357 (1988).

[88] F. Halzen and B. A. Kniehl, Nucl. Phys. **B353**, 567 (1991).

[89] F. Halzen, B. A. Kniehl, and M. L. Stong, Z. Phys. C **58**, 119 (1993).

[90] B. A. Kniehl and A. Sirlin, Nucl. Phys. **B371**, 141 (1992).

[91] B. A. Kniehl and A. Sirlin, Phys. Rev. D **47**, 883 (1993).

[92] A. Djouadi and P. Gambino, Phys. Rev. D **49**, 3499 (1994).

[93] A. Freitas, W. Hollik, W. Walter, and G. Weiglein, Phys. Lett. B **495**, 338 (2000).

[94] M. Awramik and M. Czakon, Nucl. Phys. B, Proc. Suppl. **116**, 238 (2003).

[95] L. Avdeev, J. Fleischer, S. Mikhailov, and O. Tarasov, Phys. Lett. B **336**, 560 (1994).

[96] K. Chetyrkin, J. H. Kuhn, and M. Steinhauser, Phys. Lett. B **351**, 331 (1995).

[97] K. Chetyrkin, J. H. Kuhn, and M. Steinhauser, Phys. Rev. Lett. **75**, 3394 (1995).

[98] K. Chetyrkin, J. H. Kuhn, and M. Steinhauser, Nucl. Phys. **B482**, 213 (1996).

[99] R. Boughezal, J. Tausk, and J. van der Bij, Nucl. Phys. **B713**, 278 (2005).

[100] R. Boughezal and M. Czakon, Nucl. Phys. **B755**, 221 (2006).

[101] K. Chetyrkin, M. Faisst, J. H. Kuhn, P. Maierhofer, and C. Sturm, Phys. Rev. Lett. **97**, 102003 (2006).

[102] P. Bechtle, S. Heinemeyer, O. Stål, T. Stefaniak, and G. Weiglein, Eur. Phys. J. C **74**, 2711 (2014).

[103] O. Stål and T. Stefaniak, Proc. Sci., EPS-HEP2013 (2013) 314, [arXiv:1310.4039].

[104] P. Bechtle, S. Heinemeyer, O. Stål, T. Stefaniak, and G. Weiglein, J. High Energy Phys. 11 (2014) 039.

[105] S. Heinemeyer, S. Kraml, W. Porod, and G. Weiglein, J. High Energy Phys. 09 (2003) 075.

[106] J. Alcaraz et al. (ALEPH Collaboration, DELPHI Collaboration, L3 Collaboration, OPAL Collaboration, LEP Electroweak Working Group), arXiv:hep-ex/0612034.

[107] T. Aaltonen et al. (CDF Collaboration), Phys. Rev. Lett. **108**, 151803 (2012).

[108] V. M. Abazov et al. (D0 Collaboration), Phys. Rev. D **89**, 012005 (2014).

[109] G. Bozzi, J. Rojo, and A. Vicini, Phys. Rev. D **83**, 113008 (2011).

[110] C. Bernaciak and D. Wackeroth, Phys. Rev. D **85**, 093003 (2012).

[111] M. Baak et al., arXiv:1310.6708.

[112] D. Ross and M. Veltman, Nucl. Phys. **B95**, 135 (1975).

[113] M. Veltman, Acta Phys. Polon. B **8**, 475 (1977).

[114] M. Veltman, Nucl. Phys. **B123**, 89 (1977).

[115] M. Einhorn, D. Jones, and M. Veltman, Nucl. Phys. **B191**, 146 (1981).

[116] I. Y. Kobzarev, L. Okun, and M. Voloshin, Sov. J. Nucl. Phys. **20**, 644 (1975).

[117] T. Kibble, J. Phys. A **9**, 1387 (1976).

[118] T. Kibble, Phys. Rep. **67**, 183 (1980).

[119] J. Preskill, S. P. Trivedi, F. Wilczek, and M. B. Wise, Nucl. Phys. **B363**, 207 (1991).

[120] S. Abel, S. Sarkar, and P. White, Nucl. Phys. **B454**, 663 (1995).

[121] C. Panagiotakopoulos and K. Tamvakis, Phys. Lett. B **446**, 224 (1999).

[122] V. Barger, P. Langacker, M. McCaskey, M. Ramsey-Musolf, and G. Shaughnessy, Phys. Rev. D **79**, 015018 (2009).

[123] L. Basso, S. Moretti, and G. M. Pruna, Phys. Rev. D **83**, 055014 (2011).

[124] L. Basso, S. Moretti, and G. M. Pruna, J. High Energy Phys. 08 (2011) 122.

[125] Particle Data Group, J. Beringer et al., Phys. Rev. D **86**, 010001 (2012).

[126] T. Hahn, Comput. Phys. Commun. **140**, 418 (2001).

[127] T. Hahn and M. Pérez-Victoria, Comput. Phys. Commun. **118**, 153 (1999).

[128] M. Bohm, H. Spiesberger, and W. Hollik, Fortsch. Phys. **34**, 687 (1986).

[129] A. Denner, Fortsch. Phys. **41**, 307 (1993).

[130] T. Robens and T. Stefaniak (unpublished).

[131] J. van der Bij and F. Hoogeveen, Nucl. Phys. **B283**, 477 (1987).

[132] R. Barbieri, M. Beccaria, P. Ciafaloni, G. Curci, and A. Vicere, Nucl. Phys. **B409**, 105 (1993).

[133] J. Fleischer, O. Tarasov, and F. Jegerlehner, Phys. Lett. B **319**, 249 (1993).

[134] M. Baak, M. Goebel, J. Haller, A. Hoecker, D. Kennedy, R. Kogler, K. Mönig, M. Schott, and J. Stelzer, Eur. Phys. J. C **72**, 2205 (2012).

[135] L. Lyons, D. Gibaut, and P. Clifford, Nucl. Instrum. Methods Phys. Res., Sect. A **270**, 110 (1988).

[136] P. Bechtle, O. Brein, S. Heinemeyer, O. Stål, T. Stefaniak, G. Weiglein, and K. E. Williams, Eur. Phys. J. C **74**, 2693 (2014).

[137] CMS Collaboration, CERN Report No. CMS-PAS-HIG-13-002, 2013 (unpublished).

[138] CMS Collaboration, CERN Report No. CMS-PAS-HIG-12-045, 2012 (unpublished).

[139] CMS Collaboration, CERN Report No. CMS-PAS-HIG-13-003, 2013 (unpublished).

[140] CERN Report No. ATLAS-CONF-2014-009, 2014 (unpublished).

[141] CMS Collaboration, CERN Report No. CMS-PAS-HIG-13-005, 2013 (unpublished).

[142] G. Isidori, A. V. Manohar, and M. Trott, Phys. Lett. B **728**, 131 (2014).

[143] M. Gonzalez-Alonso and G. Isidori, Phys. Lett. B **733**, 359 (2014).

[144] G. Isidori and F. Teubert, Eur. Phys. J. Plus **129**, 40 (2014).

[145] H. Flächer, M. Goebel, J. Haller, A. Hoecker, K. Mönig, and J. Stelzer, Eur. Phys. J. C **60**, 543 (2009).